iScience

CellPress
OPEN ACCESS

Article

Legionella pneumophila modulates macrophage functions through epigenetic reprogramming via the C-type lectin receptor Mincle

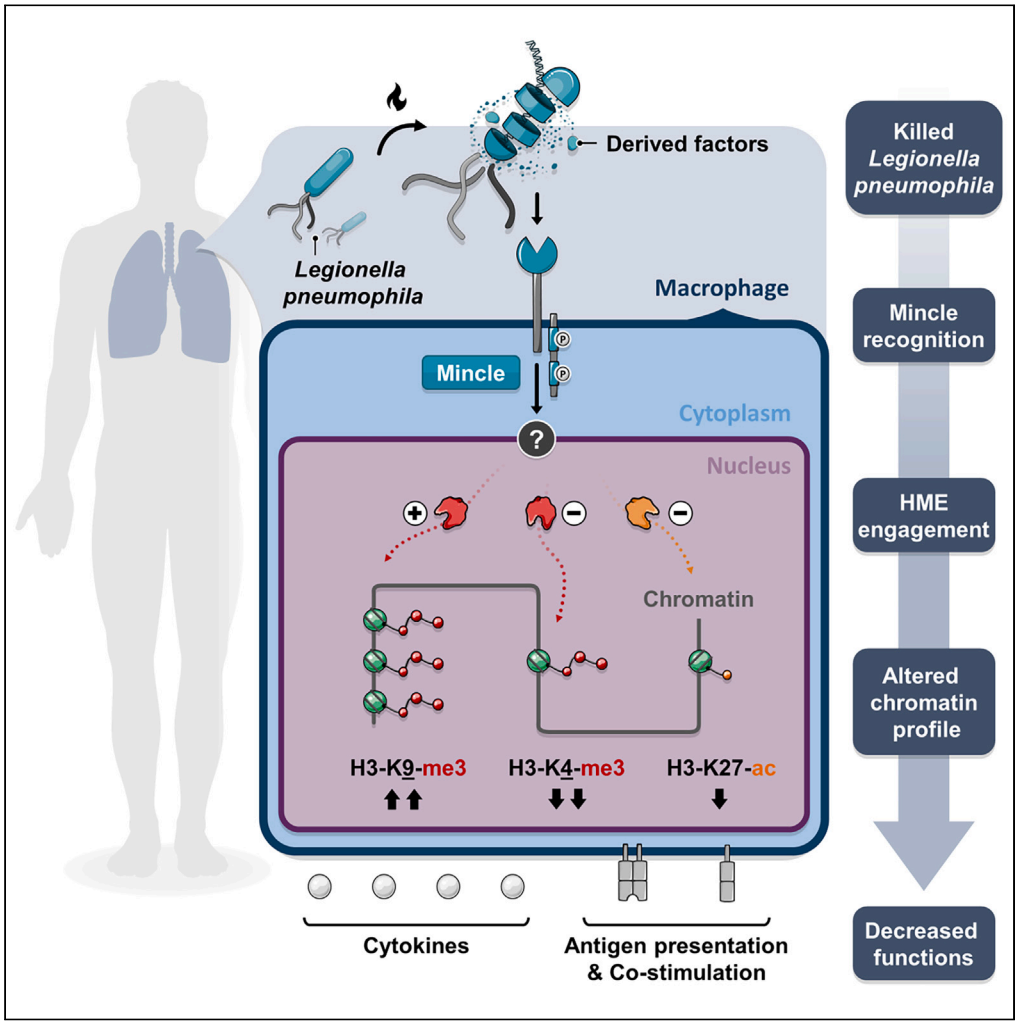

Felix Stegmann, Christina Diersing, Bernd Lepenies

bernd.lepenies@tiho-hannover.de

Highlights

L. pneumophila-derived factors reprogram macrophages into a tolerogenic state

Their epigenetic state is characterized by increased H3K9me3 and decreased H3K4me3

The C-type lectin receptor Mincle is crucial for mediating tolerance induction

Stegmann et al., iScience 27, 110700
September 20, 2024
https://doi.org/10.1016/j.isci.2024.110700

iScience

CellPress
OPEN ACCESS

Article

Legionella pneumophila modulates macrophage functions through epigenetic reprogramming via the C-type lectin receptor Mincle

Felix Stegmann,[1,2] Christina Diersing,[1,2] and Bernd Lepenies[1,2,3,*]

SUMMARY

***Legionella pneumophila* is a pathogen which can lead to a severe form of pneumonia in humans known as Legionnaires disease after replication in alveolar macrophages. Viable *L. pneumophila* actively secrete effector molecules to modulate the host's immune response. Here, we report that *L. pneumophila*-derived factors reprogram macrophages into a tolerogenic state, a process to which the C-type lectin receptor Mincle (CLEC4E) markedly contributes. The underlying epigenetic state is characterized by increases of the closing mark H3K9me3 and decreases of the opening mark H3K4me3, subsequently leading to the reduced secretion of the cytokines TNF, IL-6, IL-12, the production of reactive oxygen species, and cell-surface expression of MHC-II and CD80 upon re-stimulation. In summary, these findings provide important implications for our understanding of Legionellosis and the contribution of Mincle to reprogramming of macrophages by *L. pneumophila*.**

INTRODUCTION

Legionella pneumophila is a naturally occurring facultative intracellular pathogen in amebae which can lead to a severe form of pneumonia in humans known as Legionnaires disease[1] with a mortality rate of approximately 10%.[2] Upon inhalation of contaminated aerosols from water systems,[3] *L. pneumophila* infect alveolar macrophages within the pulmonary environment.

Recognition of *L. pneumophila* by macrophages is versatile, mostly orchestrated by a range of pattern recognition receptors (PRRs) detecting various bacterial components.[4] Several Toll-like receptors (TLRs), including TLR2, TLR5, and TLR9 play different roles in this context. For instance, TLR2 is involved in recognizing bacterial lipopeptides and *L. pneumophila*'s atypical lipopolysaccharide (LPS), characterized by a highly hydrophobic lipid A with long-chain fatty acid acylation and an O-antigen-specific chain composed of homopolymeric legionaminic acid.[5–7] TLR5 and TLR9 contribute to *L. pneumophila* recognition by detecting bacterial flagellin and enhancing neutrophil recruitment to the *L. pneumophila*-infected lung, particularly during the early stages of infection.[8,9] NOD1 and NOD2 recognize cytosolic peptidoglycan and initiate signaling through the activation of receptor-interacting protein kinase 2 (RIP2), ultimately leading to nuclear factor κB (NF-κB) activation.[10] Retinoic acid-inducible gene-I (RIG-I)-like helicases (RLHs), including melanoma differentiation-associated gene-5 (MDA5) and RIG-I, also contribute by recognition of cytosolic nucleic acids.[10] The NAIP5/NLRC4 inflammasome is responsible for detecting bacterial flagellin and plays a pivotal role in restricting replication of *L. pneumophila* in macrophages.[11,12]

C-type lectin receptors (CLRs) are PRRs that often recognize pathogen-derived glycoconjugate structures.[13] The macrophage inducible Ca^{2+}-dependent lectin receptor (Mincle; CLEC4E) was shown to recognize *Mycobacteria*,[14] *Klebsiella*,[15] *Streptococci*,[16] *Lactobacilli*[17] as well as *Helicobacter*[18] among others. Currently, little is known about the involvement of CLRs in *L. pneumophila* recognition and *L. pneumophila*-induced innate responses.

L. pneumophila regulates effector functions of infected innate immune cells[19] that are otherwise initiated to combat the pathogen. Tumor necrosis factor (TNF) enhances the phagocytosis of *Legionella* by macrophages and promotes the production of other pro-inflammatory cytokines and chemokines to recruit additional immune cells to the site of infection.[20] Likewise, interleukin (IL)-12 drives the production of interferons (IFNs) in various immune cells.[21] Type I IFN signaling restricts *L. pneumophila* replication in macrophages and lung epithelial cells, while IFN-γ-activated macrophages produce nitric oxide (NO) and inhibit bacterial replication in multiple host-cell types.[22–24] In contrast, IL-10 was shown to reverse IFN-γ-mediated inhibition of *L. pneumophila* replication in human monocytes and murine bone-marrow-derived macrophages (BMMs).[25,26] However, *L. pneumophila* secreted effectors such as Lgt1-3, SidL, LegK4, and RavX were shown to affect the host's protein synthesis, thereby strongly influencing cytokine production during infection. Infected macrophages are unable to produce sufficient amounts of TNF, IL-6, and IL-12.[27] In such cases, the host heavily relies on the production of said effector molecules by bystander cells to limit the infection.[28]

[1]Institute for Immunology, University of Veterinary Medicine Hannover, 30559 Hanover, Lower Saxony, Germany
[2]Research Center for Emerging Infections and Zoonoses, University of Veterinary Medicine Hannover, 30559 Hanover, Lower Saxony, Germany
[3]Lead contact
*Correspondence: bernd.lepenies@tiho-hannover.de
https://doi.org/10.1016/j.isci.2024.110700

L. pneumophila secreted nucleomodulins are effector proteins that access the host-cell nucleus and alter the host's epigenetic landscape.[29] These effector molecules are transferred into the host cell via the type IV secretion system (T4SS) and finally lead to the modification of host proteins through ubiquitination, phosphorylation, lipidation, glycosylation, (de-)AMPylation, phosphocholination, and dephosphocholination.[30] They also inhibit host protein translation by targeting eukaryotic elongation factors or translation initiation.[31,32] In lung epithelial cells infected with *L. pneumophila*, histone modifications, including acetylation and phosphorylation, occur globally at the promoters of relevant genes.[33] These changes in histone modifications influence pro-inflammatory gene expression in infected cells.[34] Just recently, two newly discovered *Legionella*-derived enzymes working closely together were identified to manipulate host gene expression called LphD and RomA.[35]

Still, currently little is known about how *Legionella*-derived factors impact the host's innate immune memory, how persistent the epigenetic changes are, and which host cell receptors are involved. To this end, we subjected macrophages to a primary and secondary *in vitro* stimulus with killed *L. pneumophila* and assessed the influence of the primary stimulus on the chromatin landscape, transcriptome, and macrophage effector functions. In cells primed with killed *L. pneumophila*, we identified a substantial reduction in the production of cytokines, reactive oxygen species (ROS), and surface markers both on the gene as well as on the protein levels, reminiscent of tolerance effects. Additionally, we observed increasingly condensed chromatin at respective transcriptional regions. We show that the CLR Mincle significantly contributes to the observed tolerance effects. In this study, we provide new insights into how *L. pneumophila*-derived factors have an impact on the hosts epigenetics, transcription, and protein synthesis in a Mincle-dependent manner and over a time span of several days.

RESULTS

Priming with h.i. *L. pneumophila* reduces critical effector functions in macrophages upon re-stimulation

Recognition of *L. pneumophila* triggers anti-bacterial defense mechanisms in macrophages, including the production of pro-inflammatory cytokines[36,37] and ROS.[36] While live (viable) *L. pneumophila* is known to modulate these functions in its host cell via secreted effectors,[4] little is known about how *Legionella*-derived factors impact the host. To investigate the influence of *L. pneumophila*-derived factors on host's innate responses, we primed BMMs with heat-inactivated (h.i.) *L. pneumophila* of different strains and subjected them to a secondary stimulus with the wild-type (WT) JR32 strain (Figure 1A). Upon initial priming of BMMs with different strains of h.i. *L. pneumophila* serotype 1 (WT JR32 and Corby as well as the LPS-mutant TF 3/1), we observed an increasing expression of the cytokines TNF, IL-6 and IL-12, ROS, and co-stimulatory molecules with increasing MOI, except for IL-10 (Figures S1A–S1G). After a defined resting period, re-seeding the cells (Figure 1A) ensured the viability of all cells (Figure S1H) as well as a consistency in cell counts prior to re-stimulation. When macrophages were re-stimulated with the same stimulus (h.i. WT JR32), we observed a marked reduction in the secretion of the pro-inflammatory cytokines TNF (Figure 1B), IL-6 (Figure 1C), and IL-12 (Figure 1D) with a lower secretion in case of previously higher MOI of *L. pneumophila* during priming. On the other hand, the secretion of the anti-inflammatory cytokine IL-10 was not affected by the previous priming (Figure 1E). A reduction was also observed for the production of ROS (Figure 1F) and the surface expression of major histocompatibility complex class II (MHC-II; Figure 1G) and CD80 (Figure 1H). Since all cells returned to the state of homeostasis (Figure S2), this finding excludes a prolonged response and clearly indicates a memory effect. Interestingly, the effects induced by the WT strains JR32 and Corby did not differ substantially from the LPS-mutant TF 3/1 strain, which is characterized by lower O-acetyl group substitution in its polysaccharide chain and thereby unable to generate a high-molecular-weight LPS.[38] This suggests that tolerance induction is independent of the regular LPS structure. Similar effects were also observed for *L. longbeachae*, suggesting that the macrophage modulation is not specific for *L. pneumophila* but is also mediated by other species of the *Legionella* genus (Figure S3). Collectively, these observations suggest that *Legionella*-derived factors of different strains are capable of modulating several effector functions in BMMs over a time span of at least 4 days.

RNA-sequencing of primed macrophages confirms the downregulation of several effector functions

To elucidate transcriptional changes leading to the observed inhibitory effects, we performed RNA-sequencing of BMMs both 4 h after priming as well as 4 h after re-stimulation (Figure 2A) to investigate the effects of priming and the influence of priming on re-stimulation. Principal-component analysis (PCA) of the transcriptome obtained from unprimed (−), primed (+), unprimed and unstimulated (−/−), unprimed and re-stimulated (−/+), and primed and re-stimulated (+/+) cells revealed distinct clusters (Figure S2A). Comparing Kyoto Encyclopedia of Genes and Genomes (KEGG) pathways in previously primed (+/+) and previously unprimed (−/+) cells (both re-stimulated), we observed that previously primed (+/+) cells displayed several cytokine- and innate immune receptor-associated pathways among the 20 topmost downregulated pathways (selected are shown in Figure 2B). The same sample of cells (+/+) also showed a strong downregulation of genes responsible for pro-inflammatory responses and chemo attraction relevant in Legionellosis including *Tnf*, *Il6*, and *Il12* (Figure 2C). Along those lines, several pro-inflammatory cytokines as well as chemokines were downregulated in previously primed cells (+/+). Notably, *Il10* was not differentially expressed (Figure 2D), thus confirming our observations at the protein level. This finding indicates that initial priming did not simply lead to a global reduction in transcription of cytokine genes but regulation is more nuanced, as IL-10 production is non-tolerizable by *L. pneumophila*-derived factors.

Since no KEGG-pathways or Gene Ontology (GO)-terms specifically for ROS and surface activation marker expression were available at the time of this investigation, we employed the Reactome database[39] for defined gene-sets to identify differentially expressed genes (DEGs) in our data. For the ROS and reactive nitrogen species (RNS; Reactome: R-MMU-1222556.1), several genes related to their production were differentially regulated after priming and *Nos3* remained as significantly downregulated after re-stimulation (Figure 2E). For surface activation markers, we used an extended list of the MHC class II antigen presentation pathway (Reactome: R-MMU-2132295.1), revealing the differential

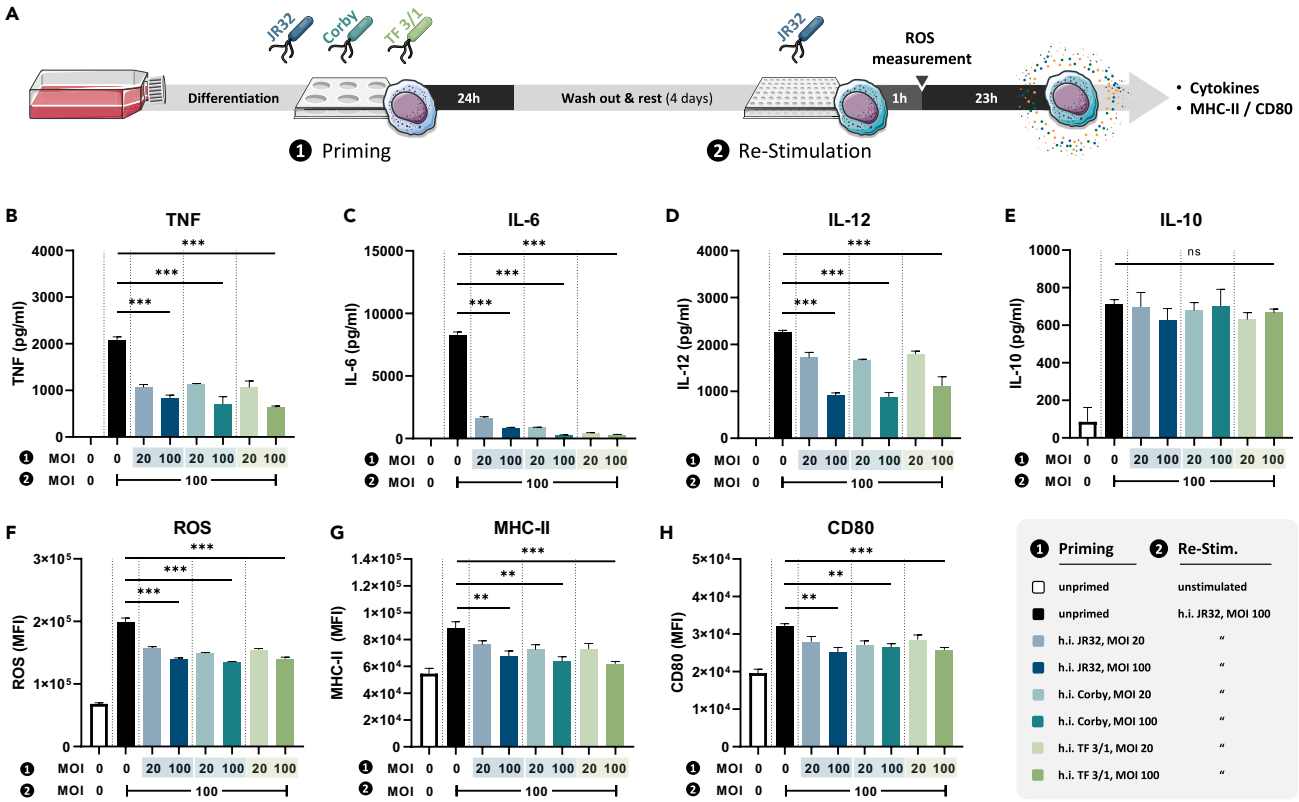

Figure 1. Prior exposure to h.i. *L. pneumophila* diminishes essential effector functions in macrophages upon subsequent re-stimulation

(A–H) (A) Schematic overview of the experimental setup. BMMs were differentiated from bone-marrow cells (BMCs) and primed with different strains of h.i. *L. pneumophila* for 24 h. Afterward, the stimulus was washed away and the cells let to rest for 4 days. Subsequently, the cells were re-seeded and re-stimulated with the h.i. JR32 strain to assess the production of selected cytokines (B–E), ROS production (F) and surface expression of MHC-II (G), and CD80 (H). Data are presented as mean +SD and are representative of three independent experiments (n = 3) in triplicates. ns = not significant, *$p < 0.05$, **$p < 0.01$, ***$p < 0.001$.

See also Figures S1–S3.

regulation of *Cd80* after priming and *H2-Ab1* (murine MHC-II) both after priming and re-stimulation (Figure 2F). Thereby, the RNA-sequencing data validated most of our protein-level observations. Notably, cytokine transcripts, including those studied at the protein level, were downregulated. Moreover, some candidates related to ROS and surface markers remained downregulated upon re-stimulation.

Interestingly, CLRs were among the highly differentially expressed pathways (Figure 2B). So far little is known about their ability to recognize *L. pneumophila*. By inquiring the KEGG CLR signaling pathway, two major candidates (LSP-1 and Mincle) could be identified (Figure 2G). For an extended overview, we also included the C-type lectin receptors reactome dataset (Reactome: R-MMU-5621481.1). The candidates which were affected by both priming and re-stimulation were *Pkd1/2*, *Cd69*, *Clec4e* (Mincle), *Vcan*, and *Sele* (Figure 2H). Notably, polycystin 1/2 (Pkd1/2), versican (Vcan), and E-selectin (Sele) are all adhesion molecules on immune cells or closely related to adhesion functionality.[40–42] Among those, Mincle not only ranked highest in significance values from RNA-sequencing but is also known to play significant roles in recognition of bacteria especially based on interactions with (glyco-)lipids.[43]

Taken together, the transcriptional profiles of BMMs indicate that *L. pneumophila*-derived factors downregulate the capacity of primed macrophages to produce transcripts of crucial importance in innate immunity during Legionellosis, including cytokines such as TNF, IL-6, and IL-12 and possibly hint at CLRs such as Mincle to be of relevance in this process.

In primed macrophages, several histone-modifying enzymes are differentially regulated

To investigate whether the observed reduced macrophage effector functions upon re-stimulation were caused by epigenetic modifications, we wanted to investigate the effect of the initial priming with killed *L. pneumophila* on histone modifying enzymes (HMEs).

From the same RNA-sequencing dataset (Figure 2A), we observed a large number of DEGs in functional GO-terms related to DNA replication and altered structure/condensation of the chromatin (Figure 3A). Upon further investigation, gene set enrichment analysis (GSEA) displayed a strong negative correlation of unprimed (–) cells with histone H3K9 modification (Figure 3B) and a strong positive correlation of previously primed and re-stimulated (+/+) macrophages with heterochromatin (Figure 3C). This suggests that the priming induces a substantial amount

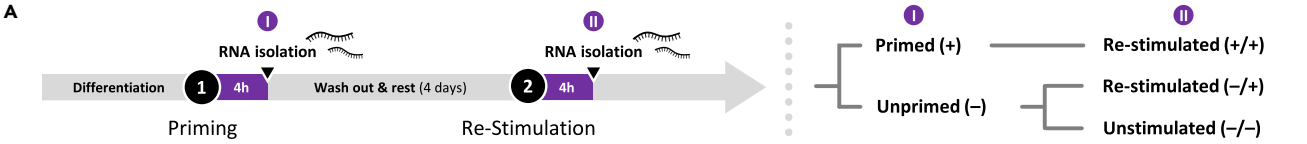

B **TOP Downregulated DEGs** (prev. primed vs. prev. unprimed)

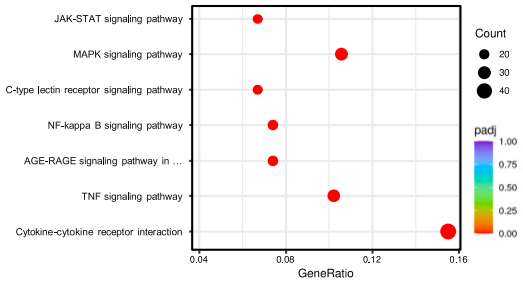

C **KEGG pathway "Legionellosis"** (prev. primed vs. prev. unprimed)

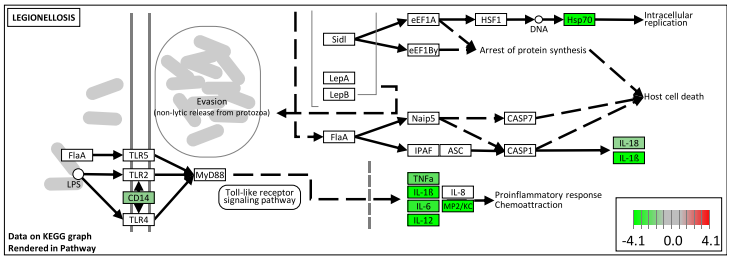

D **KEGG pathway "Cytokine-Cytokine receptor interaction"** (prev. primed vs. prev.unprimed)

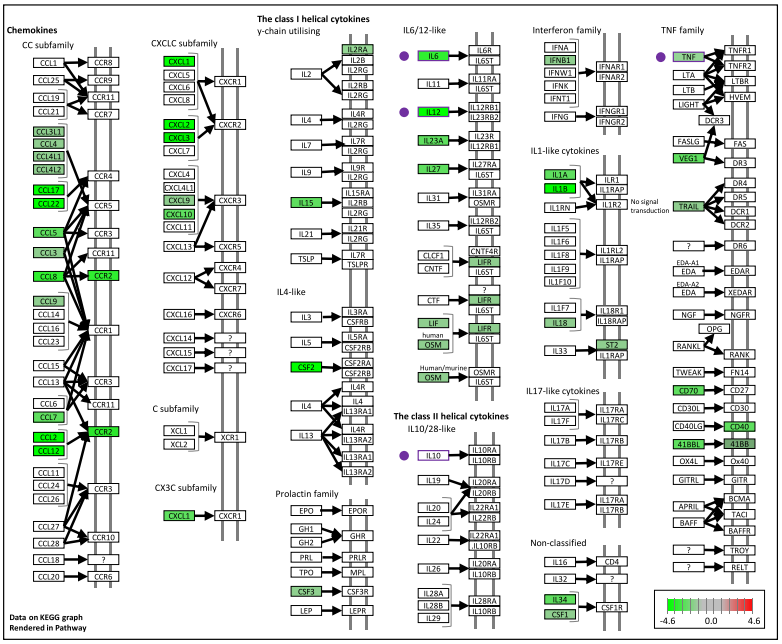

E **Reactive oxygen species**

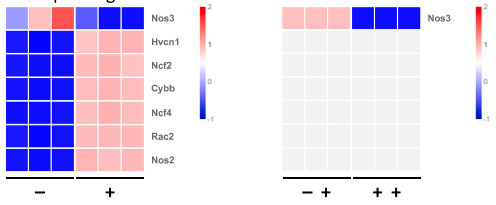

F **Surface activation markers**

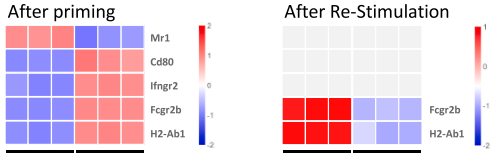

G **KEGG pathway "C-type lectin receptor signal. pathway"** (prev. primed vs. prev.unprimed)

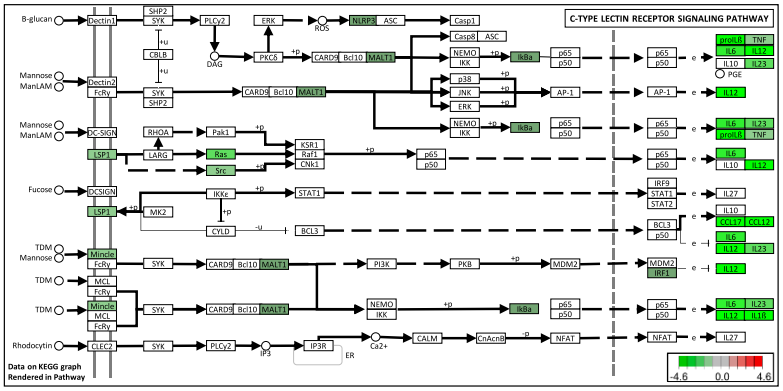

H **C-type lectins**

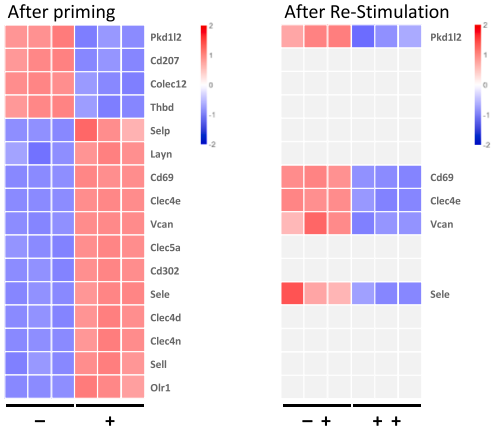

Figure 2. RNA-sequencing of previously primed macrophages shows the downregulation of numerous effector functions

(A) Time points of RNA isolation and designation of the individual samples. RNA was isolated both 4 h after priming (to compare unprimed (–) vs. primed (+)) as well as 4 h after subsequent re-stimulation (to compare previously unprimed (–/+) vs. previously primed (+/+)).

(B–H) Dot-blot of selected KEGG pathways from the TOP 20 downregulated pathways in previously primed (+/+) vs. previously unprimed (–/+) macrophages. KEGG pathway overviews of (C) Legionellosis, (D) cytokine-cytokine receptor interactions, and (G) C-type lectin receptor signaling pathway comparing previously primed (+/+) vs. previously unprimed (–/+) macrophages with several relevant genes being downregulated. Heatmaps of DEGs in the context of (E) ROS, (F) surface activation markers, and (H) C-type lectin receptors.

See also Figure S4.

of H3K9 modifications which potentially leads to a persistent heterochromatin organization, correlated with decreased gene transcription. When comparing the expression levels of genes encoding for HMEs (Reactome ID: R-MMU-3247509.1), we observed several DEGs. Notably, those HMEs upregulated in primed (+) cells contained several de-methylases, many of which have a specificity to remove H3K4me3 (Kdm5c, Kdm2b, Kdm7a, Kdm5b, and Kdm5a; Figure 3D) while HMEs which have a specificity to remove H3K9me3 (Suv39h1 and Ehmt1) were downregulated in primed (+) cells. An upregulation of H3K4me3 removing enzymes accompanied by a decrease in H3K9me3 removing enzymes might therefore hint at a general decrease in transcription activity, as large parts of the chromatin will be inaccessible for transcription factors.

Chromatin-immunoprecipitation reveals a decrease of H3K4me3 and increase of H3K9me3 in primed macrophages

To validate and extend our findings regarding the deposited epigenetic marks, we performed chromatin-immunoprecipitation (ChIP)-studies after the resting period/immediately before re-stimulation (Figure 4A). This allowed us to assess parts of the epigenetic landscape and determine whether the decrease in both transcription and/or production initially observed for TNF, IL-6, IL-12, IL-10, ROS, MHC-II, and CD80 is due to inaccessibility to their encoding genes. We observed that priming primarily increased the relative amounts of H3K9me3 (closing the chromatin) at the promoters of *Tnf*, *Il-6*, *Il-12b*, *Nox*, *Nos*, *H2-Ab1*, and *Cd80*. On top of that, the H3K4me3 mark was significantly reduced at promoters of the aforementioned genes, while a similar (although limited) effect could be seen for H3K27ac (Figure 4B).

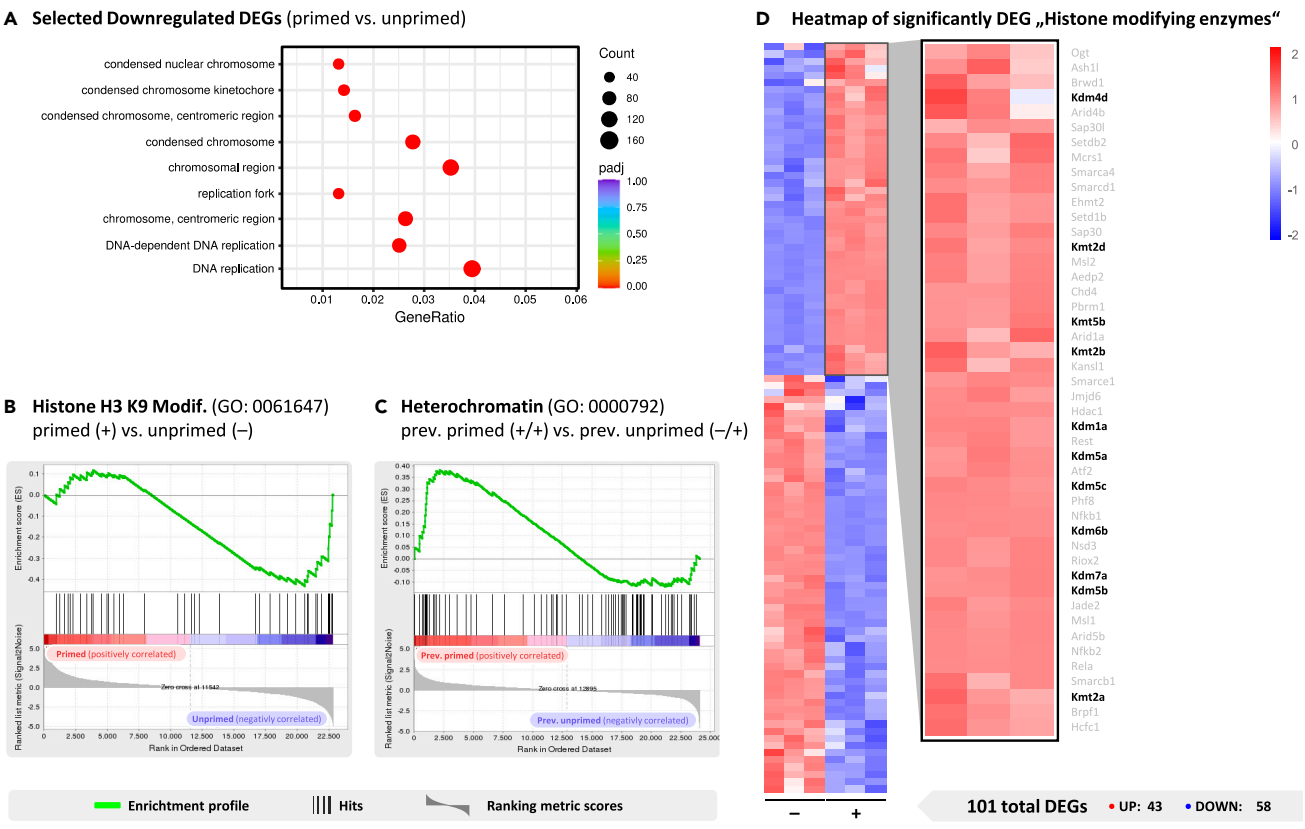

Figure 3. Within primed macrophages, there are distinct alterations in the regulation of several histone-modifying enzymes

(A–C) (A) Dot-blot of selected GO-terms from the TOP 20 DEG-sets in primed (+) vs. unprimed (–) macrophages. Selected GSEA-plots of (B) Histone H3 K9 modification in primed (+) vs. unprimed (–) macrophages and (C) Heterochromatin in previously primed (+/+) vs. previously unprimed (–/+) macrophages.

(D) Heatmap of significantly DEGs associated with HMEs comparing primed (+) vs. unprimed (–) macrophages. From this analysis, several de-methylating enzymes could be distinguished upregulated in primed (+) cells (red, upper right cluster + enlarged panel).

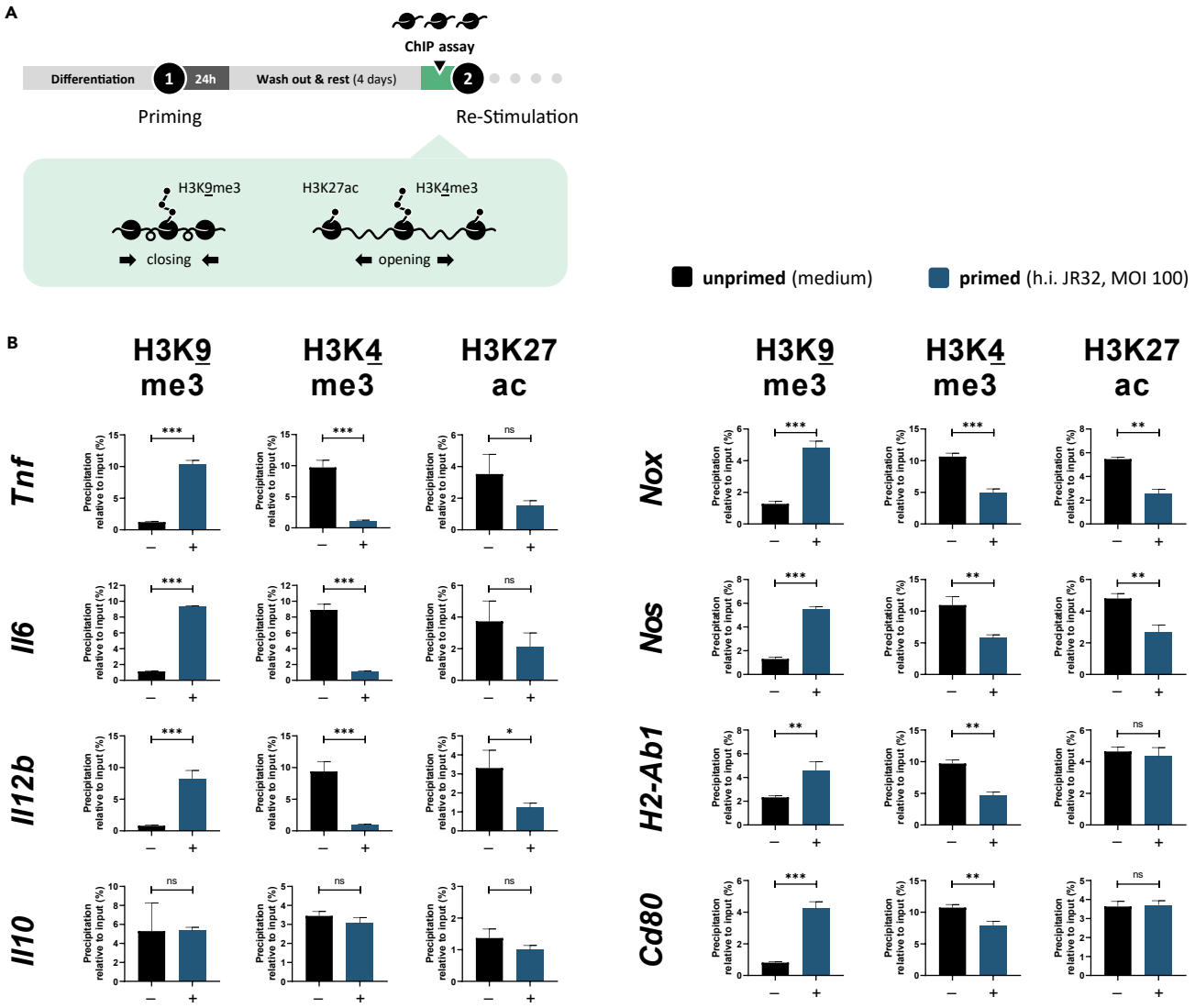

Figure 4. Chromatin-immunoprecipitation unveils a reduction in H3K4me3 and an elevation in H3K9me3 within primed macrophages

(A) Time point of chromatin isolation and subsequent ChIP assay. ChIP was performed immediately before the time point of the secondary stimulus to investigate parts of the underlying epigenetic landscape.

(B) Relative amounts of the epigenetic modifications H3K9me3 (repressive, left column), H3K4me3 (opening; middle column), H3K27ac (opening; right column) at the promoters of *Tnf*, *Il6*, *Il12b*, *Il10*, *Nox*, *Nos*, *H2-Ab1*, and *Cd80* (from top to bottom). Data are presented as mean +SD and are representative of three independent experiments ($n = 3$) in triplicates. ns = not significant, $*p < 0.05$, $**p < 0.01$, $***p < 0.001$.

Since both H3K4me3 and H3K27ac are considered to be opening marks and therefore associated with increased gene transcription, their decrease in previously primed (+) cells suggests that large regions of the chromatin in previously primed (+) cells are closed. Notably, no statistically significant differences in either H3K4me3, H3K27ac, or H3K9me3 could be observed for *Il10*, which was already unchanged on the protein- and transcriptome layer. This further suggests that the differential regulation of the observed effector functions stems from epigenetic marks changing the accessibility of the chromatin.

Taken together, the increase of H3K9me3, coupled with the decrease in H3K4me3 and H3K27ac, provide a mechanistic explanation for the decreased capacity of primed macrophages to adequately respond to secondary stimulation.

Inhibition of (de-)methylases prior to priming mitigates the *L. pneumophila* induced tolerance effect

To better understand the role of HMEs in a mechanistic way, we investigated the effect of added pan-inhibitors of methyltransferases (methylthioadhenosine; MTA), de-methylases (pargyline), acetyltransferases (epigallocatechin gallate; EGCG), and de-acetylases (Na-butyrate) on the induction of tolerance (Figure 5A).

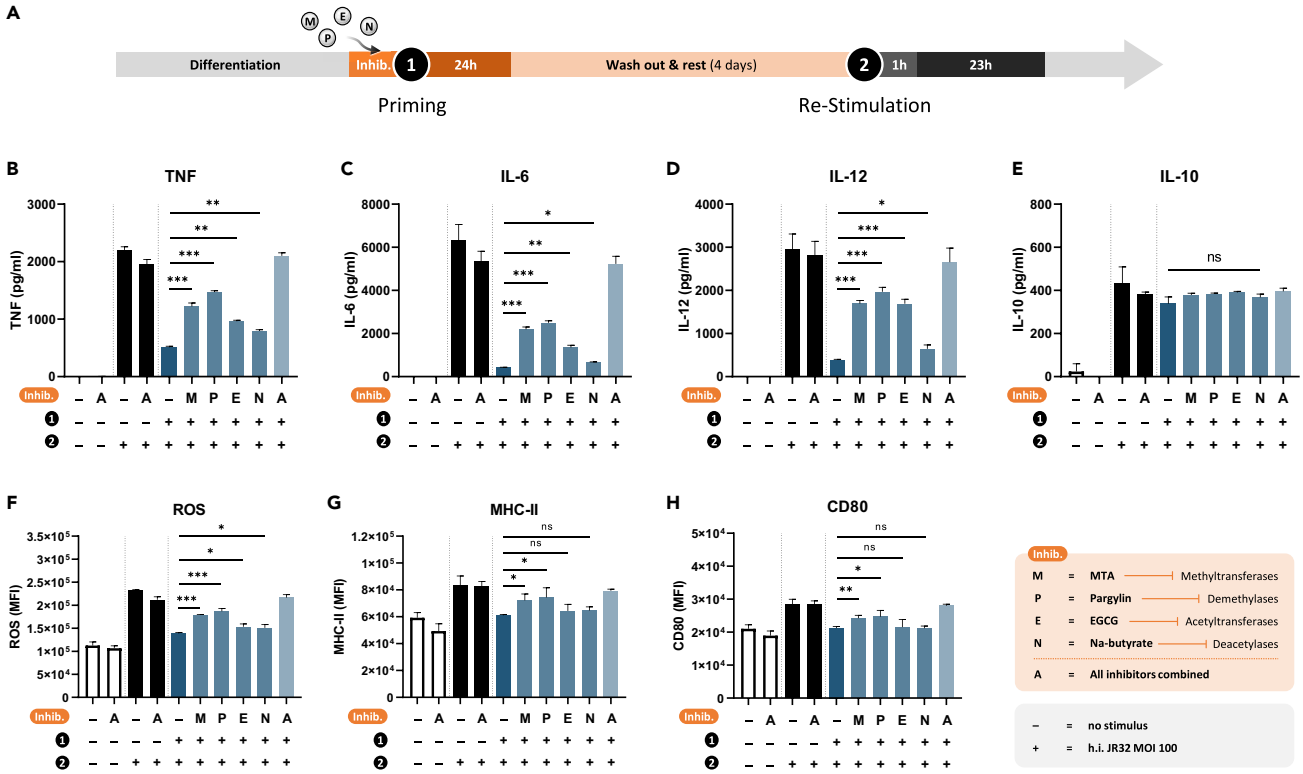

Figure 5. Pre-treatment with (de-)methylase inhibitors before priming partially alleviates the tolerance effect induced by *L. pneumophila*

(A–H) Time points and duration of pan-inhibitor treatment against methyltransferases (MTA; M), de-methylases (pargyline; P), acetyltransferases (EGCG; E), and de-acetylases (Na-butyrate; N) or all combined (A). The respective inhibitors were added prior to the priming and renewed during the resting time to investigate their impact on the readout of cytokine release (B–E), ROS production (F) and surface marker expression (G and H) after re-stimulation. Data are presented as mean +SD and are representative of three independent experiments ($n = 3$) in triplicates. ns = not significant, $*p < 0.05$, $**p < 0.01$, $***p < 0.001$.
See also Figure S5.

Out of the four inhibitors, pargyline (inhibiting de-methylases) displayed the strongest effect in mitigating the tolerance effect in expression of the cytokines TNF, IL-6, and IL-12 as well as ROS, MHC-II, and CD80 otherwise induced by the initial priming. A similar effect, albeit to a slightly lesser extent, was observed for the inhibitor MTA (inhibiting methyltransferases). Interestingly, the acetyltransferase and de-acetylase inhibitors EGCG and Na-butyrate, respectively, had significant effects on the production of TNF, IL-6, IL-12, and ROS, while H3K27ac decrease at the promoters of their respective genes was not significant in previous ChIP analysis (Figure 4B). This observation suggests that acetylations other than H3K27ac could also play a role. By combining all inhibitors, the levels of TNF, IL-6, IL-12, ROS, MHC-II, and CD80 could be restored to a level that closely resembled the previously unprimed status (Figures 5B–5H).

The inhibitor studies indicate that macrophage effector functions are regulated by epigenetic modifications by the responsible HMEs upon the initial priming. Notably, we observed a rather consistent pattern that inhibition of de-methylases (via pargyline) and methyltransferases (via MTA) had the strongest effect on modulating effector functions for most of the selected readouts, while the effects of (de-)acetylase inhibitors were weaker, most likely due to the fact that acetyl marks are generally considered less durable and may already have been degraded after four days.

The CLR Mincle markedly contributes to the *L. pneumophila* induced tolerance effect

As the CLR Mincle belonged to the strongest DEGs (Figures 2B, 2G, and 2H), we aimed at identifying the role of Mincle by subjecting WT as well as Mincle$^{-/-}$ BMMs to the same priming and re-stimulation conditions to compare their reaction regarding cytokines, ROS, and surface markers. Strikingly, Mincle$^{-/-}$ BMMs displayed a significantly less pronounced tolerance effect as determined by the secretion of the pro-inflammatory cytokines TNF (Figure 6A), IL-6 (Figure 6B), and IL-12 (Figure 6C). Additionally, the expression of MHC-II (Figure 6F) was also significantly different, while no significant differences between WT and Mincle$^{-/-}$ BMMs were observed for the production of ROS (Figure 6E) and the expression of CD80 (Figure 6G) on the surface of primed and re-stimulated macrophages when compared to their WT counterparts. To analyze whether the Mincle-mediated tolerance induction was specific for the *Legionella* genus, we tested two additional gram-negative bacteria, namely *Escherichia coli* and *Pasteurella multocida*. While we did see significant tolerance induction regarding TNF, IL-6, and IL-12 by h.i. *E. coli*, the observed tolerance effect was fully independent of the CLR Mincle. Moreover, the markedly less pronounced tolerance effects

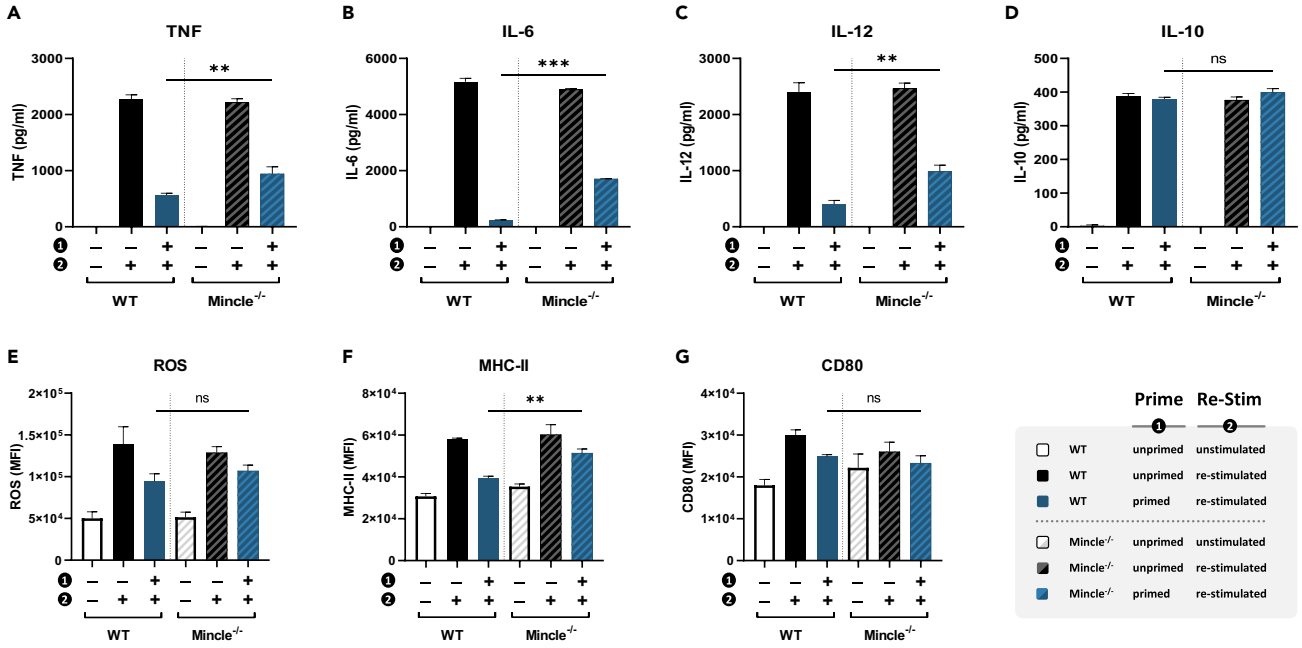

Figure 6. BMMs deficient in the CLR Mincle exhibit a milder tolerance effect induced by *L. pneumophila*

(A–G) BMMs (WT and Mincle$^{-/-}$) were primed and re-stimulated with h.i. *L. pneumophila* to determine cytokine secretion (A–D), ROS production (E) as well as surface marker expression (F and G). In most cases, primed Mincle$^{-/-}$ BMMs showed higher effector functions upon re-stimulation compared to their WT counterparts. Data are presented as mean +SD and are representative of three independent experiments (n = 3) in triplicates. ns = not significant, *$p < 0.05$, **$p < 0.01$, ***$p < 0.001$.

See also Figures S6–S8.

upon macrophage stimulation with additional unrelated bacteria such as h.i. *P. multocida* were neither dependent on Mincle (Figure S6). Therefore, neither *E. coli* LPS nor LPS from other gram-negative bacterial species demonstrated the previously observed Mincle-dependent effect.

Finally, to assess the role of Mincle in the observed reprogramming effects, we performed ChIP studies comparing WT and Mincle$^{-/-}$ BMMs focusing on the most prominent prior targets being *Tnf*, *Il6*, and *Il12b*. Indeed, we observed that lack of Mincle led to a less condensed chromatin at the promoters of *Tnf* (Figure 7A), *Il6* (Figure 7B), and *Il12b* (Figure 7C) as indicated by significantly higher levels of H3K4me3 and lower levels of H3K9me3. These results indicate that the CLR Mincle significantly contributes to the observed tolerance effects induced by killed *L. pneumophila*, thereby indicating a crucial role for Mincle in *Legionella*-induced modulation of macrophage functions.

DISCUSSION

Immunomodulation by *L. pneumophila* in macrophages is a well-documented phenomenon in the context of Legionellosis.[4,32] *L. pneumophila* secretes effector proteins to hamper host protein synthesis, thereby reducing cytokine production. T2SS secreted effector proteins are known to reduce TNF, IL-6, IL-10, IL-8, and IL-1β,[44] while T4SS secreted proteins lowered TNF, IL-6, and IL-12.[28,45] However, TSS secretion is only functional in viable *L. pneumophila*. Here, we show that factors derived from killed *Legionella* additionally induce modulation of macrophages, thereby reducing secretion of the cytokines TNF, IL-6, IL-12, the production of ROS, and presentation of MHC-II and CD80.

We show here that this modulation is mediated by *L. pneumophila*-induced epigenetic reprogramming. This conclusion is supported by the following observations: First, by RNA-sequencing, we analyzed participating pathways and saw major downregulation of transcripts encoding for crucial effector functions such as cytokines in Legionellosis like TNF, IL-6, and IL-12 and for enzymes that in return increase heterochromatin. Second, by ChIP, we observed marked increases of the closing mark H3K9me3 and decreases of the opening mark H3K4me3. Third, the use of inhibitors targeting HMEs validates the role of these enzymes in the observed immune modulation. In addition, we show that the CLR Mincle markedly contributes to the tolerogenic reaction of primed macrophages upon re-stimulation. These findings might have important implications for our understanding of Legionellosis. During infection, a large percentage of monocytes become associated with bacteria-derived material,[46] potentially interfering with monocyte development. Moreover, considering the ability of alveolar macrophages to efficiently transport other bacteria to lung-draining lymph nodes,[47] a similar phenomenon might occur with *L. pneumophila*. While this could be advantageous for initiating adaptive immune responses, it might also facilitate the dissemination of *L. pneumophila*-derived factors, contributing to immunomodulation.

Mechanistically, we have identified a central role of epigenetic reprogramming in macrophages. Here, we observed increased H3K4me3 and decreased H3K9me3 removing enzymes in RNA-sequencing (Figure 3D), while ChIP assays revealed increases in H3K9me3 and decreases

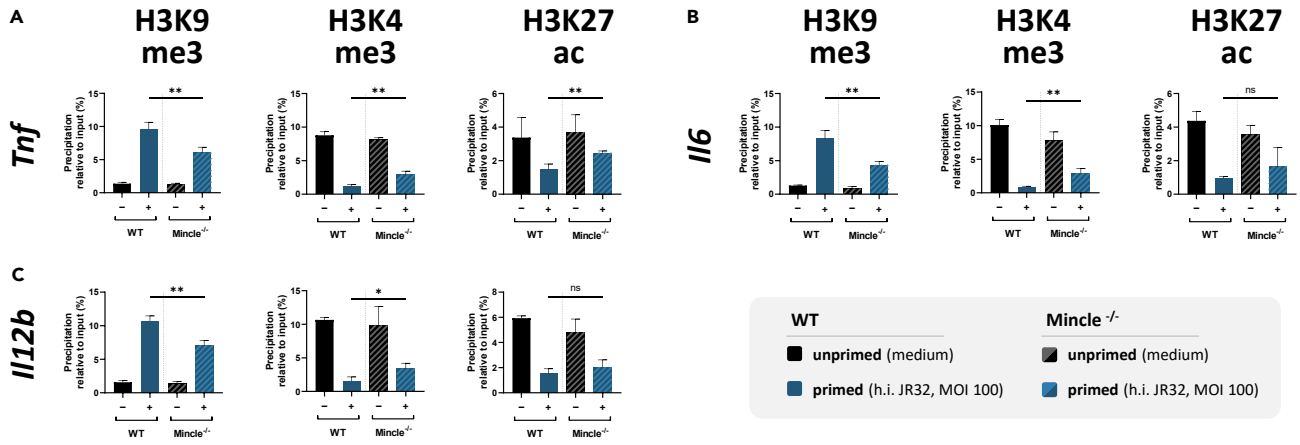

Figure 7. Chromatin-immunoprecipitation in Mincle$^{-/-}$ BMMs reveals a less condensed chromatin state at the promoters of *Tnf*, *Il6* and *Il12b*

BMMs (WT and Mincle$^{-/-}$) were primed with h.i. *L. pneumophila* and ChIP was performed prior to re-stimulation (Figure S4A). Mincle deficient BMMs displayed significantly lower amounts of H3K9me3 and higher amounts of H3K4me3 at the promoters of *Tnf*, *Il6*, and *Il12b*. Data are presented as mean +SD and are representative of three independent experiments ($n = 3$) in triplicates. ns = not significant, *$p < 0.05$, **$p < 0.01$.

in H3K4me3 (Figure 4B) which were less pronounced in the absence of Mincle (Figure 7). In inhibitor experiments, the most significant effects occurred with methyltransferase and demethylase inhibitors (Figure 5B). Tying together, these results highlight the central role of methylations for the observed effects. Earlier studies identified *L. pneumophila*-expressed flagellin to induce global, genome-wide histone modifications as well as histone H4 acetylation and H3 phosphoacetylation at the *Il8* promoter[34] and the promoter of the transcription factor ικβζ.[48] In this case, however, flagellin-mediated effects may be excluded due to the heat treatment and so are most of the other *Legionella*-derived proteins. This also renders the contribution of effectors such as RomA to the observed epigenetic reprogramming highly unlikely, which was recently described to influence the host epigenetics on a H3K14me3 basis.[35] While host-derived factors upon priming cannot be formally excluded, this leaves mainly lipids, carbohydrates, or glycolipids derived from *Legionella* to be considered. The distinct *Legionella*-derived factor(s) responsible for the epigenetic reprogramming in macrophages remain to be identified. While prior studies report similar gene-specific control of inflammation by LPS,[49] it is rather unlikely that the tolerance effects we observed are mediated by *L. pneumophila* LPS due to the following reasons: First, the structure of *L. pneumophila* LPS is different from *E. coli* LPS, marked by an extremely hydrophobic lipid A, extensively acylated with long-chain fatty acids and featuring an O-antigen-specific chain constructed from homopolymeric legionaminic acid.[7] Along those lines, we observed that tolerance induction in macrophages by h.i. *E. coli* was in fact independent of the CLR Mincle. Similarly, the less pronounced effects induced by h.i. *P. multocida* were Mincle-independent as well (Figure S6). This observation provides further evidence of the specificity of the Mincle-mediated tolerance induction by *Legionella*-derived factors. Second, both TLR4 (the classical LPS-receptor) and TLR2 (the *Legionella* LPS-receptor) were not significantly differentially expressed on the mRNA level (data not shown). Third and most importantly, we show that the TF 3/1 mutant of *L. pneumophila* displaying a truncated LPS structure still exhibits comparable effects to the WT strains JR32 and Corby. Taken together, *Legionella*-derived factors other than LPS are likely to be the responsible mediators.

In recent years, numerous studies have identified CLRs as key participants in the recognition of various pathogens and host antigenic determinants.[50] However, their specific role in *L. pneumophila* infection has not yet been elucidated. Recently, the myeloid inhibitory C-type lectin receptor (MICL; CLEC12A) was found to recognize *L. pneumophila* but had a limited role in the host's response against *L. pneumophila*.[51] Mincle has gained considerable attention as a crucial mediator in a wide array of immune interactions.[52] In recent years, the number of pathogens recognized by Mincle has significantly expanded.[53] Bacterial ligands, such as trehalose dimycolate (TDM),[14] glycerol monomycolate,[54] or β-gentiobiosyl diacylglyceride[55] from *Mycobacteria* spp., as well as monoglucosyldiacylglycerol from *Streptococcus pyogenes*[16] or the S-layer protein from *Lactobacillus brevis*[17] contribute to the recognition of the respective bacteria by Mincle. Nonetheless, the characteristics of many other ligands remain unknown and the potential interactions involving Mincle, especially with ligands from gram-negative bacteria, is not fully understood.[56] While we observed significant binding of Mincle-hFc fusion proteins to *L. pneumophila* in ELISA-based binding studies (Figure S7), a prior publication reported no significant binding to live *L. pneumophila* in a flow cytometry-based binding study.[51,57,58] This suggests that the recognized factor may not be freely accessible at the bacterial surface but is rather released upon lysis and/or heat inactivation of *Legionella*.

CLR engagement and downstream signaling is a fine-tuned balance between immune activation and repression.[13] Mincle can both stimulate and resolve inflammation and its engagement leads to the activation of the Syk/CARD9 axis.[59,60] Indeed, we saw downregulation of Mincle (Figures 2G and S8), MALT1 as part of the CARD9 complex (Figure 2G) as well as the reduction of IL-12 on several levels.

A good example for the ambivalence in Mincle signaling is demonstrated by Mincle/TDM interactions. While TDM is known to induce inflammatory reactions in macrophages upon Mincle-engagement, several reports document anti-inflammatory reactions as well.[43] For example, the Mincle/TDM interaction was reported to induce IL-10 production[18,61] or the recruitment of Src homology region 2 domain-containing phosphatase-1 (SHP-1)[53] to induce anti-inflammatory conditions.[43] The recruitment of SHP-1 by Mincle was also observed to be

exploited by ligands released in *Leishmania major* infection. In turn, this impeded the activation of antigen-presenting cells and consequently lowered initiation of adaptive immune responses.[62] Regarding IL-10 production, we did not observe any Mincle influence.

Furthermore, Mincle was reported to potentially intervene in other PRR-signaling events.[45,61,63,64] Co-stimulation of macrophages with Pam3CSK4 (a TLR2 ligand) and beads coated with TDM reduced IL-12p40 secretion.[61] Additionally, the ongoing activation of TLRs and Mincle during prolonged exposure to mycobacterial components inhibits the general translational machinery through 4EBP-1 dephosphorylation and inhibition of Nod-like receptor protein 3 (NLRP3) to reduce IL-1β production.[63] Interestingly, reduction of IL-1β was also observed in our data at least on the transcriptional level (Figures 2C and 2D) which is required to produce TNF or IL-12.[45] However, whether interference of other receptors by crosstalk plays a role in these effects remains speculative. Therefore, the exact signaling events initiated upon detection of *Legionella*-derived factors by Mincle should be unraveled in future studies.

Taken together, we provide evidence for the reprogramming of macrophage effector functions by and in response to *L. pneumophila*-derived factors. The CLR Mincle was shown to be a key component in mediating this process. Future studies should therefore elucidate the respective ligand(s) responsible for the observed effects, in particular those interacting with the CLR Mincle while also unraveling the accompanying downstream signaling.

Limitations of the study

Our study demonstrates that factors originating from *L. pneumophila* induce a shift in macrophages toward a tolerogenic state, with a significant involvement of the C-type lectin receptor Mincle (CLEC4E) in this process. While we reason that the observed responses are independent of LPS-mediated effects, the putative ligand remains elusive, which is a significant limitation of this study. Another limitation is the focus on the *L. pneumophila*-mediated modulation of effector functions in bone-marrow-derived macrophages. Future studies should investigate these effects in alveolar macrophages as they represent the primary reservoir for *L. pneumophila*.

STAR★METHODS

Detailed methods are provided in the online version of this paper and include the following:

- KEY RESOURCES TABLE
- RESOURCE AVAILABILITY
  - Lead contact
  - Materials availability
  - Data and code availability
- EXPERIMENTAL MODEL AND STUDY PARTICIPANT DETAILS
  - Animals
- METHOD DETAILS
  - Culture of Legionella pneumophila
  - Generation of bone-marrow-derived macrophages
  - Priming/re-stimulation setup
  - Inhibitor studies
  - Cytokine ELISA
  - Measurement of reactive-oxygen species
  - Activation marker and cell vitality staining
  - RNA isolation and concentration determination
  - RNA sequencing
  - RNA sequencing data analysis
  - Chromatin immunoprecipitation and ChIP-qPCR
- QUANTIFICATION AND STATISTICAL ANALYSIS

SUPPLEMENTAL INFORMATION

Supplemental information can be found online at https://doi.org/10.1016/j.isci.2024.110700.

ACKNOWLEDGMENTS

B.L. acknowledges support by the Deutsche Forschungsgemeinschaft (LE 2498/11-1, LE 2498/14-1). We thank the Hannover Graduate School for Neurosciences, Infection Medicine and Veterinary Sciences (HGNI) for supporting the PhD project of which this manuscript was a part of. We acknowledge financial support by the Open Access Fund of the University of Veterinary Medicine Hannover, Foundation. We would like to thank Bastian Opitz and Christian Lück for providing the *L. pneumophila* strains JR32, Corby and TF 3/1 as well as *L. longbeachae*. We would like to thank Hans-Joachim Schuberth and Silke Schöneberg for critical discussions and expert technical assistance, respectively. Parts of the figures use (modified) assets from Servier Medical Art. Servier Medical Art by Servier is licensed under a Creative Commons Attribution 3.0 Unported License (https://creativecommons.org/licenses/by/3.0/).

AUTHOR CONTRIBUTIONS

Conceptualization, F.S. and B.L.; methodology, F.S. and C.D.; validation, F.S., C.D., and B.L.; formal analysis, F.S.; investigation, F.S. and C.D.; resources, F.S. and C.D.; data curation, F.S.; writing – original draft, F.S. and B.L.; writing, review and editing, F.S., C.D., and B.L.; visualization, F.S.; supervision, B.L.; project administration, F.S. and B.L.; funding acquisition, B.L.

DECLARATION OF INTERESTS

The authors declare no competing interest.

Received: October 20, 2023
Revised: December 12, 2023
Accepted: August 6, 2024
Published: August 8, 2024

REFERENCES

1. Fields, B.S. (1996). The molecular ecology of legionellae. Trends Microbiol. *4*, 286–290. https://doi.org/10.1016/0966-842x(96)10041-x.
2. Phin, N., Parry-Ford, F., Harrison, T., Stagg, H.R., Zhang, N., Kumar, K., Lortholary, O., Zumla, A., and Abubakar, I. (2014). Epidemiology and clinical management of Legionnaires' disease. Lancet Infect. Dis. *14*, 1011–1021. https://doi.org/10.1016/s1473-3099(14)70713-3.
3. Kanarek, P., Bogiel, T., and Breza-Boruta, B. (2022). Legionellosis risk-an overview of Legionella spp. habitats in Europe. Environ. Sci. Pollut. Res. Int. *29*, 76532–76542. https://doi.org/10.1007/s11356-022-22950-9.
4. Chauhan, D., and Shames, S.R. (2021). Pathogenicity and Virulence of Legionella: Intracellular replication and host response. Virulence *12*, 1122–1144. https://doi.org/10.1080/21505594.2021.1903199.
5. Akamine, M., Higa, F., Arakaki, N., Kawakami, K., Takeda, K., Akira, S., and Saito, A. (2005). Differential roles of Toll-like receptors 2 and 4 in *in vitro* responses of macrophages to Legionella pneumophila. Infect. Immun. *73*, 352–361. https://doi.org/10.1128/iai.73.1.352-361.2005.
6. Girard, R., Pedron, T., Uematsu, S., Balloy, V., Chignard, M., Akira, S., and Chaby, R. (2003). Lipopolysaccharides from Legionella and Rhizobium stimulate mouse bone marrow granulocytes via Toll-like receptor 2. J. Cell Sci. *116*, 293–302. https://doi.org/10.1242/jcs.00212.
7. Luck, C., and Helbig, J.H. (2013). Characterization of legionella lipopolysaccharide. Methods Mol. Biol. *954*, 381–390. https://doi.org/10.1007/978-1-62703-161-5_24.
8. Hawn, T.R., Berrington, W.R., Smith, I.A., Uematsu, S., Akira, S., Aderem, A., Smith, K.D., and Skerrett, S.J. (2007). Altered inflammatory responses in TLR5-deficient mice infected with Legionella pneumophila. J. Immunol. *179*, 6981–6987. https://doi.org/10.4049/jimmunol.179.10.6981.
9. Bartfeld, S., Engels, C., Bauer, B., Aurass, P., Flieger, A., Brüggemann, H., and Meyer, T.F. (2009). Temporal resolution of two-tracked NF-kappaB activation by Legionella pneumophila. Cell Microbiol. *11*, 1638–1651. https://doi.org/10.1111/j.1462-5822.2009.01354.x.
10. Kawai, T., and Akira, S. (2009). The roles of TLRs, RLRs and NLRs in pathogen recognition. Int. Immunol. *21*, 317–337. https://doi.org/10.1093/intimm/dxp017.
11. Zhao, Y., Yang, J., Shi, J., Gong, Y.N., Lu, Q., Xu, H., Liu, L., and Shao, F. (2011). The NLRC4 inflammasome receptors for bacterial flagellin and type III secretion apparatus. Nature *477*, 596–600. https://doi.org/10.1038/nature10510.
12. Kofoed, E.M., and Vance, R.E. (2011). Innate immune recognition of bacterial ligands by NAIPs determines inflammasome specificity. Nature *477*, 592–595. https://doi.org/10.1038/nature10394.
13. Fischer, S., Stegmann, F., Gnanapragassam, V.S., and Lepenies, B. (2022). From structure to function - Ligand recognition by myeloid C-type lectin receptors. Comput. Struct. Biotechnol. J. *20*, 5790–5812. https://doi.org/10.1016/j.csbj.2022.10.019.
14. Ishikawa, E., Ishikawa, T., Morita, Y.S., Toyonaga, K., Yamada, H., Takeuchi, O., Kinoshita, T., Akira, S., Yoshikai, Y., and Yamasaki, S. (2009). Direct recognition of the mycobacterial glycolipid, trehalose dimycolate, by C-type lectin Mincle. J. Exp. Med. *206*, 2879–2888. https://doi.org/10.1084/jem.20091750.
15. Sharma, A., Steichen, A.L., Jondle, C.N., Mishra, B.B., and Sharma, J. (2014). Protective role of Mincle in bacterial pneumonia by regulation of neutrophil mediated phagocytosis and extracellular trap formation. J. Infect. Dis. *209*, 1837–1846. https://doi.org/10.1093/infdis/jit820.
16. Imai, T., Matsumura, T., Mayer-Lambertz, S., Wells, C.A., Ishikawa, E., Butcher, S.K., Barnett, T.C., Walker, M.J., Imamura, A., Ishida, H., et al. (2018). Lipoteichoic acid anchor triggers Mincle to drive protective immunity against invasive group A Streptococcus infection. Proc. Natl. Acad. Sci. USA *115*, E10662–E10671. https://doi.org/10.1073/pnas.1809100115.
17. Prado Acosta, M., Goyette-Desjardins, G., Scheffel, J., Dudeck, A., Ruland, J., and Lepenies, B. (2021). S-Layer From Lactobacillus brevis Modulates Antigen-Presenting Cell Functions via the Mincle-Syk-Card9 Axis. Front. Immunol. *12*, 602067. https://doi.org/10.3389/fimmu.2021.602067.
18. Devi, S., Rajakumara, E., and Ahmed, N. (2015). Induction of Mincle by Helicobacter pylori and consequent anti-inflammatory signaling denote a bacterial survival strategy. Sci. Rep. *5*, 15049. https://doi.org/10.1038/srep15049.
19. Liu, X., and Shin, S. (2019). Viewing Legionella pneumophila Pathogenesis through an Immunological Lens. J. Mol. Biol. *431*, 4321–4344. https://doi.org/10.1016/j.jmb.2019.07.028.
20. Coers, J., Vance, R.E., Fontana, M.F., and Dietrich, W.F. (2007). Restriction of Legionella pneumophila growth in macrophages requires the concerted action of cytokine and Naip5/Ipaf signalling pathways. Cell Microbiol. *9*, 2344–2357. https://doi.org/10.1111/j.1462-5822.2007.00963.x.
21. Casson, C.N., Doerner, J.L., Copenhaver, A.M., Ramirez, J., Holmgren, A.M., Boyer, M.A., Siddarthan, I.J., Rouhanifard, S.H., Raj, A., and Shin, S. (2017). Neutrophils and Ly6Chi monocytes collaborate in generating an optimal cytokine response that protects against pulmonary Legionella pneumophila infection. PLoS Pathog. *13*, e1006309. https://doi.org/10.1371/journal.ppat.1006309.
22. Nash, T.W., Libby, D.M., and Horwitz, M.A. (1988). IFN-gamma-activated human alveolar macrophages inhibit the intracellular multiplication of Legionella pneumophila. J. Immunol. *140*, 3978–3981.
23. Bhardwaj, N., Nash, T.W., and Horwitz, M.A. (1986). Interferon-gamma-activated human monocytes inhibit the intracellular multiplication of Legionella pneumophila. J. Immunol. *137*, 2662–2669.
24. Spörri, R., Joller, N., Albers, U., Hilbi, H., and Oxenius, A. (2006). MyD88-dependent IFN-gamma production by NK cells is key for control of Legionella pneumophila infection. J. Immunol. *176*, 6162–6171. https://doi.org/10.4049/jimmunol.176.10.6162.
25. Park, D.R., and Skerrett, S.J. (1996). IL-10 enhances the growth of Legionella pneumophila in human mononuclear phagocytes and reverses the protective effect of IFN-gamma: differential responses of blood monocytes and alveolar macrophages. J. Immunol. *157*, 2528–2538.
26. Yoshizawa, S., Tateda, K., Matsumoto, T., Gondaira, F., Miyazaki, S., Standiford, T.J., and Yamaguchi, K. (2005). Legionella pneumophila evades gamma interferon-mediated growth suppression through interleukin-10 induction in bone marrow-derived macrophages. Infect. Immun. *73*, 2709–2717. https://doi.org/10.1128/iai.73.5.2709-2717.2005.
27. Fontana, M.F., Banga, S., Barry, K.C., Shen, X., Tan, Y., Luo, Z.Q., and Vance, R.E. (2011). Secreted bacterial effectors that inhibit host protein synthesis are critical for induction of

the innate immune response to virulent Legionella pneumophila. PLoS Pathog. *7*, e1001289. https://doi.org/10.1371/journal.ppat.1001289.

28. Asrat, S., Dugan, A.S., and Isberg, R.R. (2014). The frustrated host response to Legionella pneumophila is bypassed by MyD88-dependent translation of pro-inflammatory cytokines. PLoS Pathog. *10*, e1004229. https://doi.org/10.1371/journal.ppat.1004229.
29. Rolando, M., Silvestre, C.D., Gomez-Valero, L., and Buchrieser, C. (2022). Bacterial methyltransferases: from targeting bacterial genomes to host epigenetics. Microlife *3*, uqac014. https://doi.org/10.1093/femsml/uqac014.
30. Rolando, M., and Buchrieser, C. (2012). Post-translational modifications of host proteins by Legionella pneumophila: a sophisticated survival strategy. Future Microbiol. *7*, 369–381. https://doi.org/10.2217/fmb.12.9.
31. Hubber, A., and Roy, C.R. (2010). Modulation of host cell function by Legionella pneumophila type IV effectors. Annu. Rev. Cell Dev. Biol. *26*, 261–283. https://doi.org/10.1146/annurev-cellbio-100109-104034.
32. Rolando, M., and Buchrieser, C. (2014). Legionella pneumophila type IV effectors hijack the transcription and translation machinery of the host cell. Trends Cell Biol. *24*, 771–778. https://doi.org/10.1016/j.tcb.2014.06.002.
33. Schmeck, B., N'Guessan, P.D., Ollomang, M., Lorenz, J., Zahlten, J., Opitz, B., Flieger, A., Suttorp, N., and Hippenstiel, S. (2007). Legionella pneumophila-induced NF-kappaB- and MAPK-dependent cytokine release by lung epithelial cells. Eur. Respir. J. *29*, 25–33. https://doi.org/10.1183/09031936.00141005.
34. Schmeck, B., Lorenz, J., N'Guessan, P.D., Opitz, B., van Laak, V., Zahlten, J., Slevogt, H., Witzenrath, M., Flieger, A., Suttorp, N., and Hippenstiel, S. (2008). Histone acetylation and flagellin are essential for Legionella pneumophila-induced cytokine expression. J. Immunol. *181*, 940–947. https://doi.org/10.4049/jimmunol.181.2.940.
35. Schator, D., Mondino, S., Berthelet, J., Di Silvestre, C., Ben Assaya, M., Rusniok, C., Rodrigues-Lima, F., Wehenkel, A., Buchrieser, C., and Rolando, M. (2023). Legionella para-effectors target chromatin and promote bacterial replication. Nat. Commun. *14*, 2154. https://doi.org/10.1038/s41467-023-37885-z.
36. Ziltener, P., Reinheckel, T., and Oxenius, A. (2016). Neutrophil and Alveolar Macrophage-Mediated Innate Immune Control of Legionella pneumophila Lung Infection via TNF and ROS. PLoS Pathog. *12*, e1005591. https://doi.org/10.1371/journal.ppat.1005591.
37. Skerrett, S.J., Bagby, G.J., Schmidt, R.A., and Nelson, S. (1997). Antibody-mediated depletion of tumor necrosis factor-alpha impairs pulmonary host defenses to Legionella pneumophila. J. Infect. Dis. *176*, 1019–1028. https://doi.org/10.1086/516530.
38. Palusinska-Szysz, M., Luchowski, R., Gruszecki, W.I., Choma, A., Szuster-Ciesielska, A., Lück, C., Petzold, M., Sroka-Bartnicka, A., and Kowalczyk, B. (2019). The Role of Legionella pneumophila Serogroup 1 Lipopolysaccharide in Host-Pathogen Interaction. Front. Microbiol. *10*, 2890. https://doi.org/10.3389/fmicb.2019.02890.
39. Gillespie, M., Jassal, B., Stephan, R., Milacic, M., Rothfels, K., Senff-Ribeiro, A., Griss, J., Sevilla, C., Matthews, L., Gong, C., et al. (2022). The reactome pathway knowledgebase 2022. Nucleic Acids Res. *50*. D687-d692. https://doi.org/10.1093/nar/gkab1028.
40. Kim, S., Nie, H., Nesin, V., Tran, U., Outeda, P., Bai, C.X., Keeling, J., Maskey, D., Watnick, T., Wessely, O., and Tsiokas, L. (2016). The polycystin complex mediates Wnt/Ca(2+) signalling. Nat. Cell Biol. *18*, 752–764. https://doi.org/10.1038/ncb3363.
41. Wight, T.N., Kang, I., Evanko, S.P., Harten, I.A., Chang, M.Y., Pearce, O.M.T., Allen, C.E., and Frevert, C.W. (2020). Versican-A Critical Extracellular Matrix Regulator of Immunity and Inflammation. Front. Immunol. *11*, 512. https://doi.org/10.3389/fimmu.2020.00512.
42. Davies, J.M., Radford, K.J., Begun, J., Levesque, J.P., and Winkler, I.G. (2021). Adhesion to E-selectin primes macrophages for activation through AKT and mTOR. Immunol. Cell Biol. *99*, 622–639. https://doi.org/10.1111/imcb.12447.
43. Miyake, Y., and Yamasaki, S. (2020). Immune Recognition of Pathogen-Derived Glycolipids Through Mincle. Adv. Exp. Med. Biol. *1204*, 31–56. https://doi.org/10.1007/978-981-15-1580-4_2.
44. McCoy-Simandle, K., Stewart, C.R., Dao, J., DebRoy, S., Rossier, O., Bryce, P.J., and Cianciotto, N.P. (2011). Legionella pneumophila type II secretion dampens the cytokine response of infected macrophages and epithelia. Infect. Immun. *79*, 1984–1997. https://doi.org/10.1128/iai.01077-10.
45. Copenhaver, A.M., Casson, C.N., Nguyen, H.T., Duda, M.M., and Shin, S. (2015). IL-1R signaling enables bystander cells to overcome bacterial blockade of host protein synthesis. Proc. Natl. Acad. Sci. USA *112*, 7557–7562. https://doi.org/10.1073/pnas.1501289112.
46. Brown, A.S., Yang, C., Fung, K.Y., Bachem, A., Bourges, D., Bedoui, S., Hartland, E.L., and van Driel, I.R. (2016). Cooperation between Monocyte-Derived Cells and Lymphoid Cells in the Acute Response to a Bacterial Lung Pathogen. PLoS Pathog. *12*, e1005691. https://doi.org/10.1371/journal.ppat.1005691.
47. Kirby, A.C., Coles, M.C., and Kaye, P.M. (2009). Alveolar macrophages transport pathogens to lung draining lymph nodes. J. Immunol. *183*, 1983–1989. https://doi.org/10.4049/jimmunol.0901089.
48. Lorenz, J., Zahlten, J., Pollok, I., Lippmann, J., Scharf, S., N'Guessan, P.D., Opitz, B., Flieger, A., Suttorp, N., Hippenstiel, S., and Schmeck, B. (2011). Legionella pneumophila-induced IκBζ-dependent expression of interleukin-6 in lung epithelium. Eur. Respir. J. *37*, 648–657. https://doi.org/10.1183/09031936.00200009.
49. Foster, S.L., Hargreaves, D.C., and Medzhitov, R. (2007). Gene-specific control of inflammation by TLR-induced chromatin modifications. Nature *447*, 972–978. https://doi.org/10.1038/nature05836.
50. Richardson, M.B., and Williams, S.J. (2014). MCL and Mincle: C-Type Lectin Receptors That Sense Damaged Self and Pathogen-Associated Molecular Patterns. Front. Immunol. *5*, 288. https://doi.org/10.3389/fimmu.2014.00288.
51. Klatt, A.B., Diersing, C., Lippmann, J., Mayer-Lambertz, S., Stegmann, F., Fischer, S., Caesar, S., Fiocca Vernengo, F., Hönzke, K., Hocke, A.C., et al. (2023). CLEC12A Binds to Legionella pneumophila but Has No Impact on the Host's Antibacterial Response. Int. J. Mol. Sci. *24*, 3891. https://doi.org/10.3390/ijms24043891.
52. Geijtenbeek, T.B.H., and Gringhuis, S.I. (2009). Signalling through C-type lectin receptors: shaping immune responses. Nat. Rev. Immunol. *9*, 465–479. https://doi.org/10.1038/nri2569.
53. Patin, E.C., Orr, S.J., and Schaible, U.E. (2017). Macrophage Inducible C-Type Lectin As a Multifunctional Player in Immunity. Front. Immunol. *8*, 861. https://doi.org/10.3389/fimmu.2017.00861.
54. Hattori, Y., Morita, D., Fujiwara, N., Mori, D., Nakamura, T., Harashima, H., Yamasaki, S., and Sugita, M. (2014). Glycerol monomycolate is a novel ligand for the human, but not mouse macrophage inducible C-type lectin, Mincle. J. Biol. Chem. *289*, 15405–15412. https://doi.org/10.1074/jbc.M114.566489.
55. Richardson, M.B., Torigoe, S., Yamasaki, S., and Williams, S.J. (2015). Mycobacterium tuberculosis β-gentiobiosyl diacylglycerides signal through the pattern recognition receptor Mincle: total synthesis and structure activity relationships. Chem. Commun. *51*, 15027–15030. https://doi.org/10.1039/c5cc04773k.
56. Miyake, Y., Ishikawa, E., Ishikawa, T., and Yamasaki, S. (2010). Self and nonself recognition through C-type lectin receptor, Mincle. Self. Nonself. *1*, 310–313. https://doi.org/10.4161/self.1.4.13736.
57. Maglinao, M., Eriksson, M., Schlegel, M.K., Zimmermann, S., Johannssen, T., Götze, S., Seeberger, P.H., and Lepenies, B. (2014). A platform to screen for C-type lectin receptor-binding carbohydrates and their potential for cell-specific targeting and immune modulation. J. Contr. Release *175*, 36–42. https://doi.org/10.1016/j.jconrel.2013.12.011.
58. Mayer, S., Moeller, R., Monteiro, J.T., Ellrott, K., Josenhans, C., and Lepenies, B. (2018). C-Type Lectin Receptor (CLR)-Fc Fusion Proteins As Tools to Screen for Novel CLR/Bacteria Interactions: An Exemplary Study on Preselected Campylobacter jejuni Isolates. Front. Immunol. *9*, 213. https://doi.org/10.3389/fimmu.2018.00213.
59. Ostrop, J., and Lang, R. (2017). Contact, Collaboration, and Conflict: Signal Integration of Syk-Coupled C-Type Lectin Receptors. J. Immunol. *198*, 1403–1414. https://doi.org/10.4049/jimmunol.1601665.
60. Rivera, A. (2014). When PRRs collide: mincle meddles with dectin and toll. Cell Host Microbe *15*, 397–399. https://doi.org/10.1016/j.chom.2014.03.013.
61. Patin, E.C., Willcocks, S., Orr, S., Ward, T.H., Lang, R., and Schaible, U.E. (2016). Mincle-mediated anti-inflammatory IL-10 response counter-regulates IL-12 *in vitro*. Innate Immun. *22*, 181–185. https://doi.org/10.1177/1753425916636671.
62. Iborra, S., Martínez-López, M., Cueto, F.J., Conde-Garrosa, R., Del Fresno, C., Izquierdo, H.M., Abram, C.L., Mori, D., Campos-Martín, Y., Reguera, R.M., et al. (2016). Leishmania Uses Mincle to Target an Inhibitory ITAM Signaling Pathway in Dendritic Cells that Dampens Adaptive Immunity to Infection. Immunity *45*, 788–801. https://doi.org/10.1016/j.immuni.2016.09.012.
63. Lee, W.B., Kang, J.S., Choi, W.Y., Zhang, Q., Kim, C.H., Choi, U.Y., Kim-Ha, J., and Kim, Y.J. (2016). Mincle-mediated translational

regulation is required for strong nitric oxide production and inflammation resolution. Nat. Commun. *7*, 11322. https://doi.org/10.1038/ncomms11322.

64. Wevers, B.A., Kaptein, T.M., Zijlstra-Willems, E.M., Theelen, B., Boekhout, T., Geijtenbeek, T.B.H., and Gringhuis, S.I. (2014). Fungal engagement of the C-type lectin mincle suppresses dectin-1-induced antifungal immunity. Cell Host Microbe *15*, 494–505. https://doi.org/10.1016/j.chom.2014.03.008.

65. Lück, P.C., Freier, T., Steudel, C., Knirel, Y.A., Luneberg, E., Zahringer, U., and Helbig, J.H. (2001). A point mutation in the active site of Legionella pneumophila O-acetyltransferase results in modified lipopolysaccharide but does not influence virulence. Int. J. Med. Microbiol. *291*, 345–352. https://doi.org/10.1078/1438-4221-00140.

66. Kostarnoy, A.V., Gancheva, P.G., Lepenies, B., Tukhvatulin, A.I., Dzharullaeva, A.S., Polyakov, N.B., Grumov, D.A., Egorova, D.A., Kulibin, A.Y., Bobrov, M.A., et al. (2017). Receptor Mincle promotes skin allergies and is capable of recognizing cholesterol sulfate. Proc. Natl. Acad. Sci. USA *114*. E2758-e2765. https://doi.org/10.1073/pnas.1611665114.

67. Dahl, J.A., and Collas, P. (2008). A rapid micro chromatin immunoprecipitation assay (microChIP). Nat. Protoc. *3*, 1032–1045. https://doi.org/10.1038/nprot.2008.68.

STAR★METHODS

KEY RESOURCES TABLE

REAGENT or RESOURCE	SOURCE	IDENTIFIER
Antibodies		
anti-H3K27ac	Diagenode	CAT#C15210016; RRID:AB_2904604
anti-H3K4me3 antibody	Diagenode	CAT#C15410003; RRID: AB_2924768
anti-H3K9me3 antibody	Diagenode	CAT#C15210014; RRID:AB_3068324
anti-Histone H3 antibody	Abcam	CAT#ab1791; RRID:AB_302613
anti-mouse CD11b APC	eBiosciences	CAT#17-0112-81; RRID:AB_469343
anti-mouse CD16/32	Biolegend	CAT#101302; RRID:AB_312801
anti-mouse CD80 PE (clone 16-10A1	Biolegend	CAT#104707; RRID:AB_313128
anti-mouse MHC-2 FITC (clone AF6-120.1,	BD Biosciences	CAT#553551; RRID:AB_394918
rabbit IgG antibody	Diagenode	CAT#C15410206; RRID:AB_2722554
Chemicals, peptides, and recombinant proteins		
7-AAD viability staining solution	ThermoFisher	CAT#00-6993-50
ACES buffer	Carl Roth	CAT#9138.2
Activated charcoal	Carl Roth	CAT#X865.1
Agar	Carl Roth	CAT#2266.3
Chelex-100 (Bio-Rad	Bio-Rad	CAT#1421253
C-type lectin receptor Fc fusion proteins	Maglinao M. (2014)[57] Klatt A. B. (2023)[51] Mayer S. (2018)[58]	N/A
Dihydrorhodamine (DHR)-123	Sigma-Aldrich	CAT#D1054-2MG
Dynabeads protein A	Invitrogen	CAT#10002D
Epigallocatechin gallate (EGCG)	Sigma-Aldrich	CAT#324880
Ferric nitrate	Carl Roth	CAT#CN84.1
L-Cysteine	Carl Roth	CAT#3467.2
Lipopolysaccharide	Sigma-Aldrich	CAT#L4391-1MG
Methylthioadhenosine (MTA)	Sigma-Aldrich	CAT#D5011
Na-butyrate	Roth	CAT#1441.1
Pargyline	Sigma-Aldrich	CAT#P8013
Phenylmethansulfonylfluorid (PMSF)	Sigma-Aldrich	CAT#P7626
Phorbol-12-myristate-13-acetate (PMA)	AppliChem	CAT#A0903,0001
Protease inhibitor mix	Sigma-Aldrich	CAT#535140
Proteinase K	ThermoFisher	CAT#EO0491
QIAzol lysis reagent	QIAgen	CAT#79306
Yeast extract	Carl Roth	CAT#2363.3
Critical commercial assays		
Murine IL-10 Standard ABTS ELISA Development Kit	Peprotech	CAT#900-K53
Murine IL-12 Standard ABTS ELISA Development Kit	Peprotech	CAT#900-K97
Murine IL-6 Standard TMB ELISA Development Kit	R&D Systems	CAT#DY-406-05
Murine TNF Standard TMB ELISA Development Kit	R&D Systems	CAT#DY-410-05
Qubit broad range assay kit	FischerSci	CAT#Q10210
RNeasy mini kit	QIAgen	CAT#74104
SYBR Green based Luna qPCR Master mix	NEB	CAT#M3003X

(*Continued on next page*)

Continued

REAGENT or RESOURCE	SOURCE	IDENTIFIER
Experimental models: Organisms/strains		
L. pneumophila serotype 1 strain Corby	Lück P. C. (2001)[65]	N/A
L. pneumophila serotype 1 strain JR32	Lück P. C. (2001)[65]	N/A
L. pneumophila serotype 1 strain TF 3/1	Lück P. C. (2001)[65]	N/A
L. longbeachae	Gift from the Charité Berlin	N/A
E. coli	Gift from the TiHo Institute for Microbiology	N/A
P. multocida	National Collection of Type Cultures (NCTC)	CAT#10322
Mincle$^{-/-}$ mice	Kostarnoy A.V. (2017)[66]	N/A
Oligonucleotides		
Mincle primers	ThermoFisher Scientific	CAT#Mm01183703_m1
18S primers	ThermoFisher Scientific	CAT#Mm03928990_g1
For ChIP-qPCR primers, please refer to Table S1		
Deposited data		
RNA-sequencing dataset	This study	SRA: PRJNA1030160
Software and algorithms		
BD Accuri C6 Plus Software	BD Biosciences	N/A
FlowJo Version 10	FlowJo LLC	N/A
GraphPad Prism Version 7	GraphPad Software	N/A

RESOURCE AVAILABILITY

Lead contact

Further information, data and request for resources and reagents should be directed to and will be fulfilled by the Lead Contact, Bernd Lepenies (Bernd.Lepenies@tiho-hannover.de).

Materials availability

This study did not generate new unique reagents.

Data and code availability

- RNA sequencing data have been deposited at SRA and are publicly available as of the date of publication. Accession numbers are listed in the key resources table.
- This paper does not report original code.
- Any additional information is available from the lead contact upon request.

EXPERIMENTAL MODEL AND STUDY PARTICIPANT DETAILS

Animals

All mice were housed in the animal facility of the University of Veterinary Medicine (Hannover, Germany) in individually ventilated cages under controlled conditions (12 h light/12 h dark cycle, 22-24°C, humidity 50-60 %) and specific pathogen-free conditions with permanent access to water and standard rodent feed. The source of the Mincle$^{-/-}$ mice (generated by the Consortium for Functional Glycomics) was described previously.[66] Sacrificing of mice for scientific purposes was approved by the Animal Welfare Officers of the University of Veterinary Medicine Hannover (AZ 02.05.2016, TiHo-T-2019-13, TiHo-T-2024-6). Bone marrow cells were isolated from female WT or Mincle$^{-/-}$ mice (C57BL/6 background, aged 8 to 16 weeks).

METHOD DETAILS

Culture of Legionella pneumophila

The *L. pneumophila* wildtype (WT) strain JR32, belonging to serogroup type I, alongside the WT Corby strain and its isogenic LPS-mutant TF 3/1 were included in the study.[65] The isogenic mutant TF 3/1 was generously provided by Dr. Christian Lück from the Technische Universität Dresden and both the JR32 and Corby strain were obtained from Dr. Bastian Opitz from the Charité Berlin. All *L. pneumophila* strains were

cultivated on buffered charcoal yeast extract (BCYE) agar plates for a duration of two days at 37°C. For experimental investigations, bacterial cultures were grown in a medium containing N-(2-acetamido)-2-aminoethanesulfonic acid (ACES)-buffered yeast extract (AYE) and were subsequently subjected to two washes with PBS. L-cysteine and ferric nitrate supplements were added to both the BCYE agar plates and the AYE medium. The heat-inactivation (h.i.) process was carried out at 75°C for one hour and its effectiveness was confirmed by plating the bacteria on BCYE agar.

Generation of bone-marrow-derived macrophages

Bone marrow cells from both WT or Mincle$^{-/-}$ (C57BL/6 background) were isolated from the tibia and femur of female mice aged 8 to 16 weeks. The bones were cleaned with 70 % ethanol followed by flushing using IMDM supplemented with 10 % FCS, 2 mM L-glutamine, and 100 U/mL penicillin/streptomycin. The resulting cell mixture was filtered through a 40 μm cell strainer and then subjected to centrifugation at 300 × g for 5 minutes. To remove red blood cells, a solution of 90 % 160 mM NH_4Cl and 10 % 100 mM Tris-HCl (pH 7.5) was used. The bone marrow cells were then washed and preserved at -150°C using a 10 % DMSO solution. To induce the differentiation to BMMs, the bone marrow cells were cultured in a BMM differentiation medium, comprising IMDM, 10 % FCS, 30 % L929 fibroblast supernatant, 4.5 mM L-glutamine, and 100 μg/mL penicillin/streptomycin. On the second and fourth day of cultivation, fresh medium was introduced.

Priming/re-stimulation setup

BMMs for the priming/re-stimulation setup were cultured as described above. On day 5 of culture, 3 x 10^5 cells/well in 1 ml BMM differentiation medium were seeded into a 6-well flat bottom plate to attach and rest for minimum 1 h. Afterwards, the medium was renewed and BMMs were primed with the indicated amounts of h.i. *L. pneumophila*. After 24 h, the stimulant was removed and the cells were rinsed twice with pre-warmed PBS and fresh BMM differentiation medium was added to start a resting period of 4 days. At the end of the resting period, BMMs were detached, centrifuged and counted to allow re-seeding of equal amounts (1 x 10^5 cells/well in 100 μl) in a 96-well plate for re-stimulation experiments. Re-seeded cells were stimulated with the indicated amounts of h.i. *L. pneumophila* for either 1 h (ROS) or 24 h (activation markers, cytokines) and the cytokine containing supernatant was stored at -80°C (Figure 1A).

Inhibitor studies

For inhibitor studies, culture of BMMs and read-outs were performed as described above with the exception to adding the inhibitors methylthioadhenosine (MTA; 500 μM), pargyline (5 μM), epigallocatechin gallate (EGCG; 50 μM), Na-butyrate (100 μM) or a combination of all during the priming and resting period.

Cytokine ELISA

Culture supernatants acquired subsequent to priming/stimulation of BMMs were analyzed for the presence of various cytokines. TNF and IL-6 were assessed using DuoSet ELISA kits (R&D Systems) while IL-12 and IL-10 was evaluated using the ABTS ELISA Development Kit (PeproTech) according to the respective manufacturer's instructions. The plates were developed using the substrate 3,3′,5,5′-Tetramethylbenzidine (TMB) or 2,2′-azino-bis-3-ethylbenzothiazoline-6-sulfonic acid (ABTS), respectively. To quantify the results, absorbance readings were taken at 450 nm with a wavelength correction at 570 nm or 405 nm with a wavelength correction at 650 nm, respectively, using a TECAN infinite M1000 spectrophotometer (TECAN).

Measurement of reactive-oxygen species

After re-seeding of the BMMs into a 96-well round bottom plate as described above, cells were incubated for a minimum amount of 2 h to attach and rest. Afterwards, the supernatant was removed and a mixture of IMDM, DHR123 and stimulant (h.i. *L. pneumophila* or 10 mM PMA as positive control) was added. After an incubation of 1 h, the samples were put on ice until the measurement of reactive oxygen species (ROS) by flow cytometry (Accuri flow cytometer, BD Biosciences) and data were analyzed using the BD Accuri™ C6 software (BD Biosciences).

Activation marker and cell vitality staining

After re-seeding of the BMMs into a 96-well round bottom plate as described above, BMMs were blocked using anti-mouse CD16/32 (clone 93, eBioscience; 1:100) for 10 minutes at 4°C. Subsequently, the cells were stained with APC-conjugated anti-mouse CD11b (clone M1/70, eBiosciences; 1:200), PE-conjugated anti-mouse CD80 (clone 16-10A1, Biolegend; 1:200), and FITC-conjugated anti-mouse MHC-2 (clone AF6-120.1, BD Pharmingen; 1:200) for 20 minutes at 4°C. Following this staining, the cells were incubated with 1 % paraformaldehyde (PFA). To determine the cell vitality, unfixed cells were incubated with the cell vitality dye 7AAD (Thermofisher; 1:80) and incubated for 15 min before measurement. Cells treated with intense UV-light for 20 min and a 50:50 mixture of viable and UV-treated cells served as controls. Flow cytometry analysis was performed using the Accuri flow cytometer (BD Biosciences). Data analysis of the obtained results was performed using the BD Accuri™ C6 software (BD Biosciences).

RNA isolation and concentration determination

Total RNA for sequencing was isolated 4 h after priming or re-stimulation, respectively (Figure 2A). Briefly, the cells were centrifuged at 300 xg for 5 min and washed twice with ice-cold PBS. Next, the cells were lysed using QIAzol (QIAgen) and purified using RNeasy kits (QIAgen)

according to the manufacturer's instructions. The concentration and integrity of the isolated RNA was determined using the Qubit broad range assay kit (Invitrogen). Isolated total RNA was sent to Novogene Co, Ltd. for sequencing and subsequent data analysis.

RNA sequencing

RNA sequencing as well as data analysis was performed by Novogene Co, Ltd. The methodological descriptions provided are summarized in the following paragraphs.

Library preparation for transcriptome sequencing

Messenger RNA was purified from total RNA using poly-T oligo-attached magnetic beads. After fragmentation, the first strand cDNA was synthesized using random hexamer primers, followed by the second strand cDNA synthesis using either dUTP for directional library or dTTP for non-directional library. The non-directional library was ready after end repair, A-tailing, adapter ligation, size selection, amplification, and purification. The directional library was ready after end repair, A tailing, adapter ligation, size selection, USER enzyme digestion, amplification, and purification. The library was checked with Qubit and real-time PCR for quantification and bioanalyzer for size distribution detection. Quantified libraries were pooled and sequenced on Illumina platforms, according to effective library concentration and data amount.

Clustering and sequencing

The clustering of the index-coded samples was performed according to the manufacturer's instructions. After cluster generation, the library preparations were sequenced on an Illumina platform and paired-end reads were generated.

RNA sequencing data analysis

Quality control

Raw data (raw reads) of fastq format were firstly processed through fastp software. In this step, clean data (clean reads) were obtained by removing reads containing adapter, reads containing poly-N and low-quality reads from raw data. At the same time, Q20, Q30 and GC contents of the clean data were calculated. All downstream analyses were based on clean data with high quality.

Reads mapping to the reference genome

Reference genome and gene model annotation files were downloaded from the UCSC genome browser website. The index of the reference genome was built using Hisat2 v2.0.5 and paired-end clean reads were aligned to the reference genome using Hisat2 v2.0.5. Hisat2 was selected as the mapping tool as Hisat2 can generate a database of splice junctions based on the gene model annotation file and thus generates a better mapping result than other non-splice mapping tools.

Quantification of gene expression level

FeatureCounts v1.5.0-p3 was used to count the reads numbers mapped to each gene. Subsequently, the FPKM of each gene was calculated based on the length of the gene and reads count mapped to this gene. FPKM, expected number of Fragments Per Kilobase of transcript sequence per Millions base pairs sequenced, considers the effect of sequencing depth and gene length for the reads count at the same time, and is currently the most commonly used method for estimating gene expression levels.

Differential expression analysis

Differential expression analysis of two conditions/groups (two biological replicates per condition) was performed using the DESeq2 R package (1.20.0). DESeq2 provide statistical routines for determining differential expression in digital gene expression data using a model based on the negative binomial distribution. The resulting P-values were adjusted using the Benjamini and Hochberg's approach for controlling the false discovery rate. Genes with an adjusted P-value less than or equal to 0.05 found by DESeq2 were assigned as differentially expressed.

GO and KEGG enrichment analysis of differentially expressed genes

Gene Ontology (GO) enrichment analysis of differentially expressed genes was implemented by the clusterProfiler R package, in which gene length bias was corrected. GO terms with corrected P-values less than 0.05 were considered significantly enriched by differential expressed genes. KEGG is a database resource for understanding high-level functions and utilities of the biological system, such as the cell, the organism and the ecosystem from molecular-level information, especially large-scale molecular datasets generated by genome sequencing and other high-throughput experimental technologies (http://www.genome.jp/kegg/). The clusterProfiler R package was used to test the statistical enrichment of differential expression genes in KEGG pathways.

Gene Set Enrichment Analysis

Gene Set Enrichment Analysis (GSEA) is a computational approach to determine if a pre-defined Gene Set can show a significant consistent difference between two biological states. The genes were ranked according to the degree of differential expression in the two samples, and then the predefined Gene Set were tested to see if they were enriched at the top or bottom of the list. Gene set enrichment analysis can

include subtle expression changes. We use the local version of the GSEA analysis tool http://www.broadinstitute.org/gsea/index.jsp, GO, KEGG data set were used for GSEA independently.

Chromatin immunoprecipitation and ChIP-qPCR

Chromatin immunoprecipitation (ChIP) was performed following a previously described method with slight modifications.[67] Briefly, a total of 3 x 10^5 cells per sample at the end of the resting period from previously primed or unprimed BMMs (Figure 4A) were initially harvested and cross-linked using 1 % formaldehyde for 8 min followed by quenching the reaction with glycine for 5 min at room temperature. Subsequently, the cross-linked cells were lysed with 120 μL of lysis buffer composed of 50 mM Tris-HCl (pH 8.0), 10 mM EDTA, 1 % (wt/vol) SDS, a protease inhibitor mix (diluted 1:100; Sigma) with additional 1 mM PMSF, and 20 mM Na-butyrate. The chromatin present within the lysate underwent sonication to generate fragments in the range of 300-500 base pairs using a Sonopuls cuphorn sonicator (Bandelin Sonopuls; 100 % power, 8x 30 sec on/off on ice). Following this, the sonicated chromatin was diluted with 800 μL of RIPA ChIP buffer, which comprised 10 mM Tris·HCl (pH 7.5), 140 mM NaCl, 1 mM EDTA, 0.5 mM EGTA, 1% (vol/vol) Triton X-100, 0.1% (wt/vol) SDS, 0.1% (wt/vol) Na-deoxycholate, a protease inhibitor mix (Sigma, diluted 1:1000), 1 mM PMSF, and 20 mM Na-butyrate.

For immunoprecipitation, Dynabeads protein A (10 μL; Invitrogen) were incubated separately with 1 μg of either anti-H3 (Abcam), anti-H3K4me3 (Diagenode), anti-H3K27ac (Diagenode) or anti-H3K9me3 antibody (Diagenode) for 2 hours with 40 rpm rotation. Additionally, a rabbit IgG antibody (Diagenode) was used as a negative control for ChIP-grade antibodies. After this pre-treatment, 100 μL of the sheared chromatin was subjected to immunoprecipitation using the antibody-bound bead complexes. Afterwards, protein-DNA complexes were eluted and purified using 10 % (w/v) chelex-100 (Bio-Rad Laboratories) in Tris-EDTA. In parallel, another 100 μL of the sheared chromatin was utilized for the separate extraction of total input DNA. Both immunoprecipitated and input DNA were purified by incubation with 20 μg proteinase K (10 mg/ml), followed by heating the samples at 100°C for 10 min and quick centrifugation to remove the DNA containing supernatant from the magnetic beads.

For the quantification of the ChIP samples, qPCR was carried out using the SYBR Green based Luna qPCR Master mix (NEB) and specific primers targeting *Tnf*, *Il6*, *Il12b*, *Il10*, *Nox*, *Nos*, *H2-Ab* and *Cd80* (for sequences see Table S1). The amount of precipitated DNA of target regions was determined relative to the input to assess the changes of epigenetic epitopes of target regions between primed and unprimed samples.

QUANTIFICATION AND STATISTICAL ANALYSIS

Except for the RNA sequencing data (described above), all analyses conducted were processed using GraphPad Prism (version 8, GraphPad Software). Paired, two-tailed Student's t-tests were employed for the analysis. In all analyses, asterisks indicate significant differences (ns = not significant, * $p < 0.05$, ** $p < 0.01$, *** $p < 0.001$).